ELSEVIER

Journal of Alloys and Compounds 262–263 (1997) 39–44

Journal of ALLOYS AND COMPOUNDS

Crystal structures of low-temperature phases (Phase II) of ionic conductors Ag_7TaS_6 and Ag_7NbS_6

M. Onoda*, H. Wada, M. Tansho, M. Ishii

National Institute for Research in Inorganic Materials, 1-1 Namiki, Tsukuba, Ibaraki 305, Japan

Abstract

The crystal structures of low-temperature forms of argyrodite-type ionic conductors, namely Ag_7TaS_6 II (between approx. 280 and 170 K) and Ag_7NbS_6 II (between approx. 280 and 140 K), have been analyzed and compared to each other using powder X-ray diffraction data. The crystal structure of Ag_7TaS_6 II could be described on the basis of a space group Pc with the lattice constants a = 7.453 Å, b = 7.403 Å, c = 12.806 Å and β = 124.62°. In the Rietveld analysis of Ag_7NbS_6 II, a commensurately modulated structure approach was adopted to obtain a smooth convergence. The crystal data are expressed as a_1 = 7.368 Å, a_2 = 14.770 Å, a_3 = 12.768 Å, σ = (0.25, 0, 0), β = 124.28° in a four-dimensional formalism with a superspace-group Pc(α, 1/2, γ), that is A = 29.47 Å, B = 14.770 Å, C = 12.768 Å, β = 124.28° in a three-dimensional formalism with a space group C2. In Ag_7TaS_6 II, three-sevenths of Ag ions are in the distorted S–S tetrahedrons and the residual four-sevenths are in the triangles shared by two tetrahedrons. On the other hand in the model of Ag_7NbS_6 II, most of a half of 28 independent Ag ions are in distorted tetrahedrons and most of the other half of Ag ions are in triangular faces shared by two tetrahedrons. © 1997 Elsevier Science S.A.

Keywords: Ionic conductors; Ag_7TaS_6; Ag_7NbS_6; Crystal structures

1. Introduction

Ternary sulfides Ag_7TaS_6 and Ag_7NbS_6 were synthesized and their Ag ion conductivities at ambient temperatures were found [1,2]. They were identified as cubic phases of the argyrodite-family [3,4] with the space group $F\bar{4}3m$, Z = 4 and a = 10.514 Å for Ag_7TaS_6 or a = 10.500 Å for Ag_7NbS_6. Silver ions are distributed statistically over many sites in the framework TaS_6 or NbS_6 composed of a tetrahedrally closed-packed S sublattice and group V transition elements [1,2]. Silver ions are considered to be disordered but correlated to each other in the room-temperature phases I, as suggested by diffuse scattering observed in each powder X-ray diffraction pattern of Ag_7TaS_6 I and Ag_7NbS_6 I [2].

The low-temperature powder X-ray diffraction experiments revealed the respective two low-temperature phases, namely Ag_7TaS_6 II (between approx. 280 and 170 K), Ag_7TaS_6 III (below approx. 170 K), Ag_7NbS_6 II (between approx. 280 and 140 K) and Ag_7NbS_6 III (below approx. 140 K) [5,6]. About the intermediate phase II of Ag_7TaS_6, the Rietveld analysis was successfully performed and the crystal structure could be described on the basis of a monoclinic system of a space group Pn with the lattice constants A = 7.453 Å, B = 7.403 Å, C = 10.540 Å and β = 90.069° which is equivalent to a space group Pc with the lattice constants A = 7.453 Å, B = 7.403 Å, C = 12.916 Å and β = 125.31° or A = 7.453 Å, B = 7.403 Å, C = 12.806 Å, β = 124.62° [7]. The pattern of

* Corresponding author.

0925-8388/97/$17.00
PII S0925-8388(97)00326-5

Table 1
Crystal data and the atomic coordinates of the phase II of Ag_7TaS_6 at 253 K

Crystal data [monoclinic, space group Pc (no. 7)]
A = 7.453 Å, B = 7.403 Å, C = 12.806Å, β = 124.62°
Coordinates of equivalent positions: x, y, z; x, −y, 1/2 + z

Atom	x	y	z	Atom	x	y	z
Ag1	0.679 (8)	0.026 (8)	0.490 (7)	Ta	0.0	0.254 (4)	0.0
Ag2	0.482 (9)	0.074 (7)	0.691 (7)	S1	0.377 (13)	0.25 (2)	0.134 (12)
Ag3	−0.147 (9)	0.353 (8)	0.652 (7)	S2	0.817 (12)	0.25 (2)	0.101 (12)
Ag4	0.474 (9)	0.489 (8)	0.765 (6)	S3	0.81 (2)	−0.002 (12)	0.866 (11)
Ag5	0.211 (10)	0.119 (6)	0.292 (6)	S4	0.87 (3)	0.497 (13)	0.847 (13)
Ag6	0.377 (9)	0.433 (6)	0.950 (6)	S5	0.24 (2)	0.24 (2)	0.77 (2)
Ag7	0.075 (9)	0.291 (7)	0.529 (9)	S6	0.47 (2)	0.26(2)	0.51 (3)

Notes: The standard deviations are listed in parentheses.
The values listed have been derived from those in Table 1 of Onoda et al. [7].

Table 2
Atomic parameters of Ag_7NbS_6 II described in the four-dimensional formalism

		x	y	z
Ag1	Fundamental	0.89	0.07	0.57
	A_0	0.010 (5)	0.007 (1)	0.013 (3)
	A_1	−0.050 (7)	0.012 (2)	0.007 (4)
	B_1	−0.025 (5)	0.012 (2)	−0.048 (3)
	A_2	0.006 (5)	0.017 (1)	−0.017 (3)
Ag2	Fundamental	0.43	0.01	0.78
	A_0	0.012 (5)	0.005 (1)	0.007 (3)
	A_1	−0.028 (5)	−0.027 (2)	0.046 (3)
	B_1	0.091 (4)	0.034 (2)	0.038 (2)
	A_2	−0.11 (2)	−0.077 (7)	0.06 (1)
Ag3	Fundamental	0.00	0.34	0.74
	A_0	0.007 (5)	0.003 (1)	−0.005 (3)
	A_1	0.044 (5)	0.023 (2)	0.023 (2)
	B_1	−0.011 (4)	−0.020 (2)	0.008 (3)
	A_2	0.022 (3)	0.000 (2)	0.031 (2)
Ag4	Fundamental	0.68	0.17	0.76
	A_0	0.001 (5)	0.002 (1)	0.002 (2)
	A_1	0.024 (5)	−0.076 (2)	−0.012 (3)
	B_1	0.016 (4)	0.028 (2)	0.009 (3)
	A_2	0.000 (7)	0.093 (3)	0.028 (4)
Ag5	Fundamental	0.37	0.17	0.27
	A_0	0.007 (5)	−0.004 (1)	0.006 (3)
	A_1	−0.107 (4)	0.020 (2)	−0.002 (3)
	B_1	−0.117 (5)	−0.065 (2)	−0.056 (3)
	A_2	0.004 (7)	−0.022 (3)	−0.148 (5)
Ag6	Fundamental	0.66	0.22	0.96
	A_0	0.012 (5)	−0.002 (1)	0.004 (2)
	A_1	−0.124 (5)	−0.008 (2)	−0.042 (3)
	B_1	0.037 (5)	−0.010 (2)	0.016 (3)
	A_2	0.122 (9)	−0.011 (4)	0.034 (5)
Ag7	Fundamental	0.25	0.20	0.58
	A_0	0.007 (4)	0.006 (1)	−0.003 (2)
	A_1	0.024 (4)	−0.021 (2)	0.012 (3)
	B_1	−0.034 (5)	0.000 (2)	0.022 (3)
	A_2	0.029 (6)	−0.013 (3)	0.000 (3)
Nb	Fundamental	0.0	0.13	0.0
	A_0	0.0	−0.012 (1)	0.0
	A_1	−0.007 (6)	−0.004 (3)	−0.006 (4)
	B_1	0.007 (7)	0.002 (3)	−0.010 (4)
	A_2	0.009 (7)	0.000 (3)	−0.002 (4)
S1	Fundamental	0.38	0.13	0.13
	A_0	0.004 (7)	−0.018 (3)	−0.020 (5)
	A_1	0.00 (1)	0.008 (6)	0.006 (6)
	B_1	0.01 (1)	0.013 (7)	−0.001 (8)
	A_2	0.01 (2)	−0.05 (1)	−0.06 (1)
S2	Fundamental	0.88	0.13	0.13
	A_0	0.04 (1)	−0.023 (4)	0.018 (7)
	A_1	−0.07 (1)	0.022 (7)	−0.027 (8)
	B_1	0.01 (2)	−0.023 (3)	−0.01 (1)
	A_2	0.03 (1)	−0.007 (4)	0.002 (7)
S3	Fundamental	0.87	0.00	0.87
	A_0	−0.007 (7)	−0.013 (3)	0.009 (4)
	A_1	−0.01 (1)	−0.003 (6)	−0.004 (7)
	B_1	0.00 (2)	0.006 (4)	−0.004 (8)
	A_2	0.00 (1)	0.003 (4)	−0.008 (6)
S4	Fundamental	0.87	0.26	0.87
	A_0	0.029 (8)	−0.005 (3)	0.028 (4)
	A_1	−0.07 (1)	0.001 (5)	−0.009 (5)
	B_1	0.01 (2)	0.004 (6)	0.008 (7)
	A_2	0.05 (5)	0.005 (5)	0.016 (5)
S5	Fundamental	0.25	0.13	0.75
	A_0	−0.005 (10)	0.012 (3)	−0.018 (5)
	A_1	−0.006 (2)	0.001 (6)	0.011 (9)
	B_1	−0.03 (1)	−0.009 (6)	0.01 (1)
	A_2	−0.01 (2)	0.013 (7)	−0.001 (7)
S6	Fundamental	0.50	0.13	0.50
	A_0	0.03 (1)	−0.020 (4)	0.021 (6)
	A_1	−0.07 (1)	−0.029 (6)	−0.029 (9)
	B_1	0.07 (1)	0.006 (6)	−0.01 (1)
	B_2	−0.06 (1)	0.017 (5)	−0.011 (7)

A_m and B_m are the amplitudes of the cosine and sine terms with wave vector $mk = ma^*/4$ in the displacive modulation function expressed as a Fourier series (a_1 = 7.368, a_2 = 14.770, a_3 = 12.768Å and β = 124.28°).

Ag_7NbS_6 II, not so similar to that of Ag_7TaS_6 II, could be indexed on the basis of a monoclinic superstructure model of the argyrodite-type, and the lattice constants are A = 4 × 7.368 Å, B = 2 × 7.389 Å, C = 12.98 Å and β = 124.28° [6].

In this study, Rietveld analysis of Ag_7NbS_6 II has been attempted based on the powder X-ray diffrac-

Table 3
Selected interatomic distances (Å) in Ag_7NbS_6 II

$Ag1_0$	$-S2_0$	2.7		$-S5_2$	2.4		$-S4_2$	2.3
	$-S3_0$	2.4	$Ag3_3$	$-S2_2$	2.2		$-S5_2$	3.0
	$-S5_1$	2.5		$-S4_2$	3.0		$-S6_2$	2.8
	$-S6_0$	2.7		$-S5_3$	2.6	$Ag6_3$	$-S2_3$	2.4
$Ag1_1$	$-S2_1$	2.7		$-S6_2$	2.9		$-S4_3$	2.4
	$-S3_1$	2.3	$Ag4_0$	$-S3_0$	2.3		$-S5_3$	2.6
	$-S4_1$	2.8		$-S4_0$	2.6	$Ag7_0$	$-S4_{-1}$	2.2
	$-S5_1$	2.3		$-S6_0$	2.8		$-S5_0$	2.2
$Ag1_2$	$-S2_2$	2.7	$Ag4_1$	$-S1_1$	2.2		$-S6_0$	2.5
	$-S3_2$	3.0		$-S3_1$	2.9	$Ag7_1$	$-S1_1$	2.5
	$-S5_3$	2.6		$-S4_1$	2.2		$-S4_0$	2.5
	$-S6_2$	2.3	$Ag4_2$	$-S3_2$	2.8		$-S5_1$	2.3
$Ag1_3$	$-S3_2$	3.0		$-S4_2$	2.2		$-S6_1$	3.1
	$-S5_3$	2.4		$-S5_2$	2.8	$Ag7_2$	$-S1_2$	2.7
	$-S6_2$	2.3		$-S6_2$	2.6		$-S4_1$	2.4
$Ag2_0$	$-S3_0$	2.9	$Ag4_3$	$-S3_3$	2.6		$-S5_2$	2.3
	$-S5_0$	2.6		$-S4_3$	2.3		$-S6_2$	3.1
	$-S6_0$	2.3		$-S5_3$	2.9	$Ag7_3$	$-S1_3$	2.5
$Ag2_1$	$-S3_1$	2.3		$-S6_3$	2.8		$-S4_2$	2.7
	$-S5_1$	2.3	$Ag5_0$	$-S1_0$	2.2		$-S5_3$	2.3
	$-S6_1$	2.8		$-S2_{-1}$	2.2		$-S6_3$	2.9
$Ag2_2$	$-S1_2$	2.3		$-S5_0$	3.1	Nb_0	$-S1_0$	2.4
	$-S2_1$	2.6	$Ag5_1$	$-S1_1$	2.3		$-S2_{-1}$	2.4
	$-S3_2$	3.0		$-S2_0$	2.7		$-S3_{-1}$	2.3
	$-S5_2$	2.4		$-S6_1$	2.8		$-S4_{-1}$	2.4
$Ag2_3$	$-S1_3$	2.4	$Ag5_2$	$-S1_2$	2.3	Nb_1	$-S1_1$	2.4
	$-S3_3$	3.0		$-S3_2$	3.1		$-S2_0$	2.3
	$-S5_3$	2.4		$-S4_2$	2.2		$-S3_0$	2.3
	$-S6_3$	2.8	$Ag5_3$	$-S5_3$	2.5		$-S4_0$	2.3
$Ag3_0$	$-S2_{-1}$	2.7		$-S6_3$	2.9	Nb_2	$-S1_2$	2.4
	$-S4_{-1}$	2.6	$Ag6_0$	$-S2_0$	2.8		$-S2_1$	2.3
	$-S5_0$	2.3		$-S4_0$	2.5		$-S3_1$	2.3
$Ag3_1$	$-S2_{-1}$	2.2		$-S5_0$	2.6		$-S4_1$	2.3
	$-S4_0$	2.9		$-S6_0$	2.4	Nb_3	$-S1_3$	2.4
	$-S5_1$	2.3	$Ag6_1$	$-S2_1$	2.6		$-S2_2$	2.3
$Ag3_2$	$-S2_1$	2.6		$-S4_1$	2.3		$-S3_2$	2.4
	$-S4_1$	2.3	$Ag6_2$	$-S2_2$	2.7		$-S4_2$	2.4

Suffixes, −1, 0, 1, 2 and 3, represent unit-cell translations along the a_1 axis, respectively.

tion data. It is difficult to obtain a smooth convergence in an ordinary Rietveld analysis in the case of a superstructure, because of overlap of many reflections. However, an application of the superspace-group theory often lead to a smooth convergence in the crystal structure refinement, and a superstructure can be regarded as a modulated structure with a commensurate wave vector. In addition, a setting of the starting parameter is expected to become simple by adopting the multi-dimensional formalism. Then we have used the computer program PREMOS for the Rietveld analysis based on the superspace-group approach [8].

2. Experimental

The details of the preparation processes and the process of low-temperature X-ray diffractometry was similar to that used previously [5,7]. Diffraction data were collected with a step-scan procedure using CuK_α radiation with a graphite-monochromator at 245 K for Ag_7NbS_6 II. No electron diffraction pattern was obtained because of unstableness of the specimen under the electron radiation.

3. Symmetry consideration and structure refinement

As discussed in the previous paper [6], a large part of the strong reflections of the phase II of Ag_7NbS_6 can be indexed from a monoclinic cell ($a' = 7.368$ Å, $b' = 7.389$ Å, $c' = 12.77$ Å and $\beta = 124.28°$). The cell is based on the axes $\boldsymbol{a}' \cong (\boldsymbol{a} + \boldsymbol{b})/2$, $\boldsymbol{b}' \cong (-\boldsymbol{a} + \boldsymbol{b})/2$ and $\boldsymbol{c}' \cong \boldsymbol{c} - (\boldsymbol{a} + \boldsymbol{b})/2$, when the basic axes $\boldsymbol{a}$, $\boldsymbol{b}$ and $\boldsymbol{c}$ are used for the cubic phase Ag_7NbS_6 I. The other peaks of Ag_7NbS_6 II are assumed to be superstructure reflections, and all peaks could be indexed from the monoclinic lattice based on $\boldsymbol{A} \cong 2(\boldsymbol{a} + \boldsymbol{b})$, $\boldsymbol{B} \cong (-\boldsymbol{a} + \boldsymbol{b})$ and $\boldsymbol{C} \cong \boldsymbol{c} - (\boldsymbol{a} + \boldsymbol{b})/2$, with the lattice constants A = 4 × 7.368 Å, B = 2 × 7.389 Å, C = 12.77 Å and $\beta = 124.28°$ and the reflection conditions $H + K = 2n$ for HKL and $L = 2n$ for $H0L$. The three-dimensional space group of Ag_7NbS_6 II is considered to be Cc (no. 9). In order to apply the four-dimensional formalism, adoption of the basic cell with the axes $\boldsymbol{a}_1 = \boldsymbol{a}' \cong (\boldsymbol{a} + \boldsymbol{b})/2$, $\boldsymbol{a}_2 = 2\boldsymbol{b}' \cong \boldsymbol{a} + \boldsymbol{b}$ and $\boldsymbol{a}_3 = \boldsymbol{c}' \cong \boldsymbol{c} - (\boldsymbol{a} + \boldsymbol{b})/2$ and the monoclinic angle $\beta = 124.28°$ is feasible to understand. The primary modulation wave vector is given by $\boldsymbol{k} = \boldsymbol{a}_1^*/4$ to describe the structure of Ag_7NbS_6 II as a commensurate modulated structure. Each reflection is expressed by $\mathbf{q} = h\boldsymbol{a}_1^* + k\boldsymbol{a}_2^* + l\boldsymbol{a}_3^* + m\boldsymbol{k} = (4h + m)(\boldsymbol{a}_1^*/4) + k\boldsymbol{a}_2^* + l\boldsymbol{a}_3^* = H\boldsymbol{A}^* + K\boldsymbol{B}^* + L\boldsymbol{C}^*$ by using four integers, h, k, l and m, where $\boldsymbol{a}_1^*$, $\boldsymbol{a}_2^*$ and $\boldsymbol{a}_3^*$ are the reciprocal vectors corresponding to $\boldsymbol{a}_1$, $\boldsymbol{a}_2$ and $\boldsymbol{a}_3$. The cell constants are $a_1 = 7.368$ Å, $a_2 = 14.770$ Å, $a_3 = 12.77$ Å, $\boldsymbol{\sigma} = (0.25, 0, 0)$ and $\beta = 124.28°$. The systematic reflection condition, $k + m = 2n$ for $hklm$ and $l = 2n$ for $h0lm$, was observed. As the condition for the main reflections is $k = 2n$ for hkl and $l = 2n$ for $h0l$, the possible space group of the fundamental structure is considered to be Pc with a duplicated axis $\boldsymbol{a}_2$. The centering translation of (0, 1/2, 0, 1/2) in a four-dimensional formalism is implied by $k + m = 2n$ for $hklm$, and then the superspace group derived is expressed as Pc(α, 1/2, γ) which is equivalent to Pb(α, β, 1/2) of the literature [9].

The starting parameters of the basic structure of Ag_7NbS_6 II have been derived from the structure of Ag_7TaS_6 II. The atomic parameters of Ag_7TaS_6 II, is based on $\beta = 124.62°$ and Pc, are derived as listed in Table 1 from the parameters, based on $\beta = 90.069°$ and the space group Pn, reported in the previous paper, [7] and the values are used to set the starting model of the Ag_7NbS_6 II.

Refinement was attempted based on the superspace group Pc(α, 1/2, γ) through a Rietveld analysis pro-

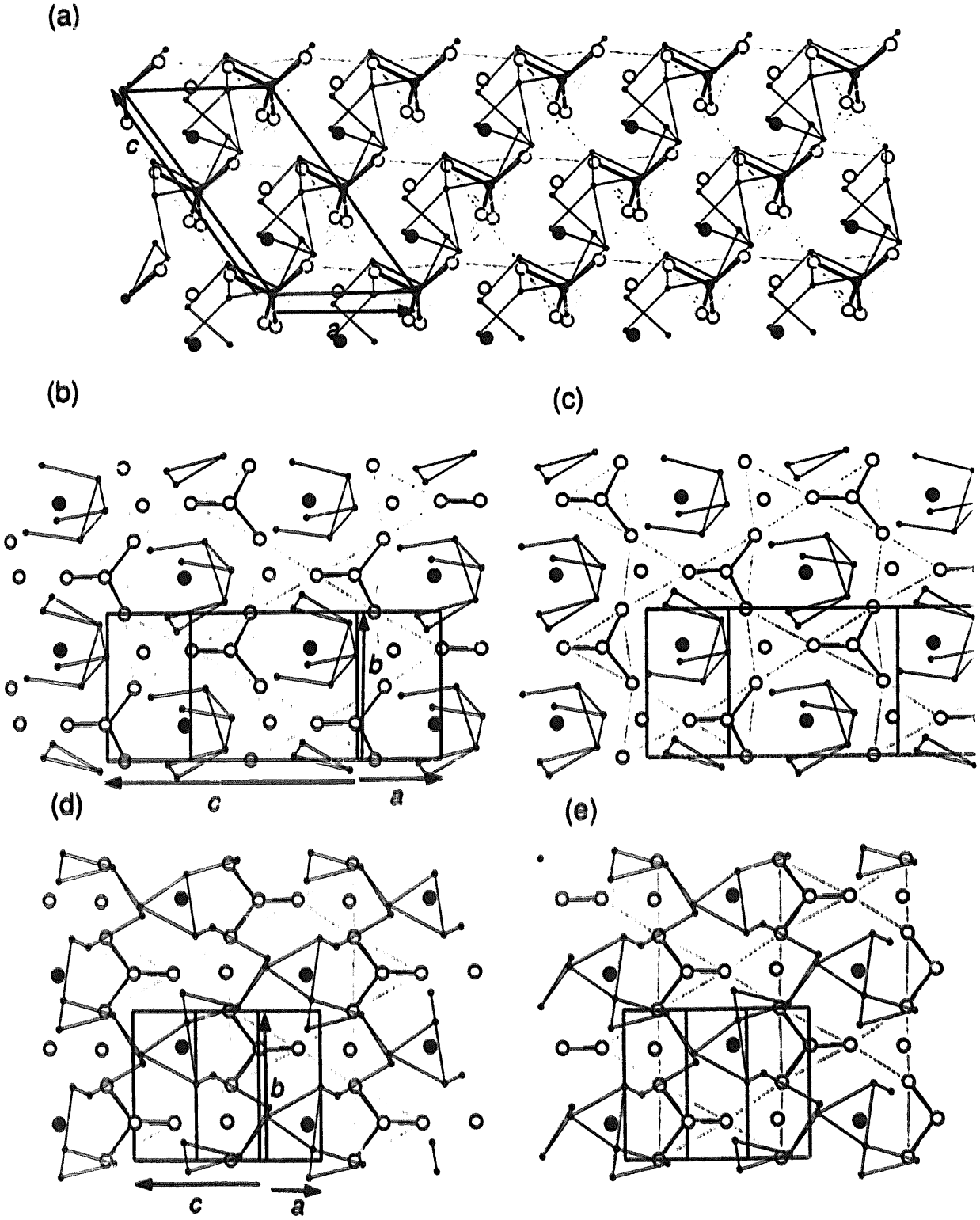

Fig. 1. Projections of the structure model of Ag_2TaS_6 II along (a) [0, 1, 0], (b,c) [−3, 0, −1], (d,e) [2, 0, −1] on the basis of the monoclinic unit cell (a = 7.453 Å, b = 7.403 Å, c = 12.806 Å and β = 124.62°). The bounded areas for (b–e) are, respectively (b) $-0.23 < x < 0.77$, (c) $0.77 < x < 1.77$, (d) $-0.65 < x - 2y < 0.35$ and (e) $0.35 < x - 2y < 1.35$. Large open and hatched circles, medium solid circles and small solid circles represent S, Ta and Ag, respectively.

gram PREMOS [8] using the powder X-ray diffraction data measured at 245 K. The Fourier amplitudes of the cosine A_m and sine B_m terms with the suffixes m representing the wave vectors $mk = ma_1^*/4$ in the displacive modulation functions were adopted as structure parameters by considering the structural degree of freedom. To suppress the excessive parameter shifts, the penalty functions included in the pro-

gram PREMOS have been used for the interatomic distances. The agreement was fairly good with 166 structural parameters; $R_{wp} = 0.094$. The final parameters are listed in Table 2.

4. Discussion

The structure models of Ag_7TaS_6 II and Ag_7NbS_6

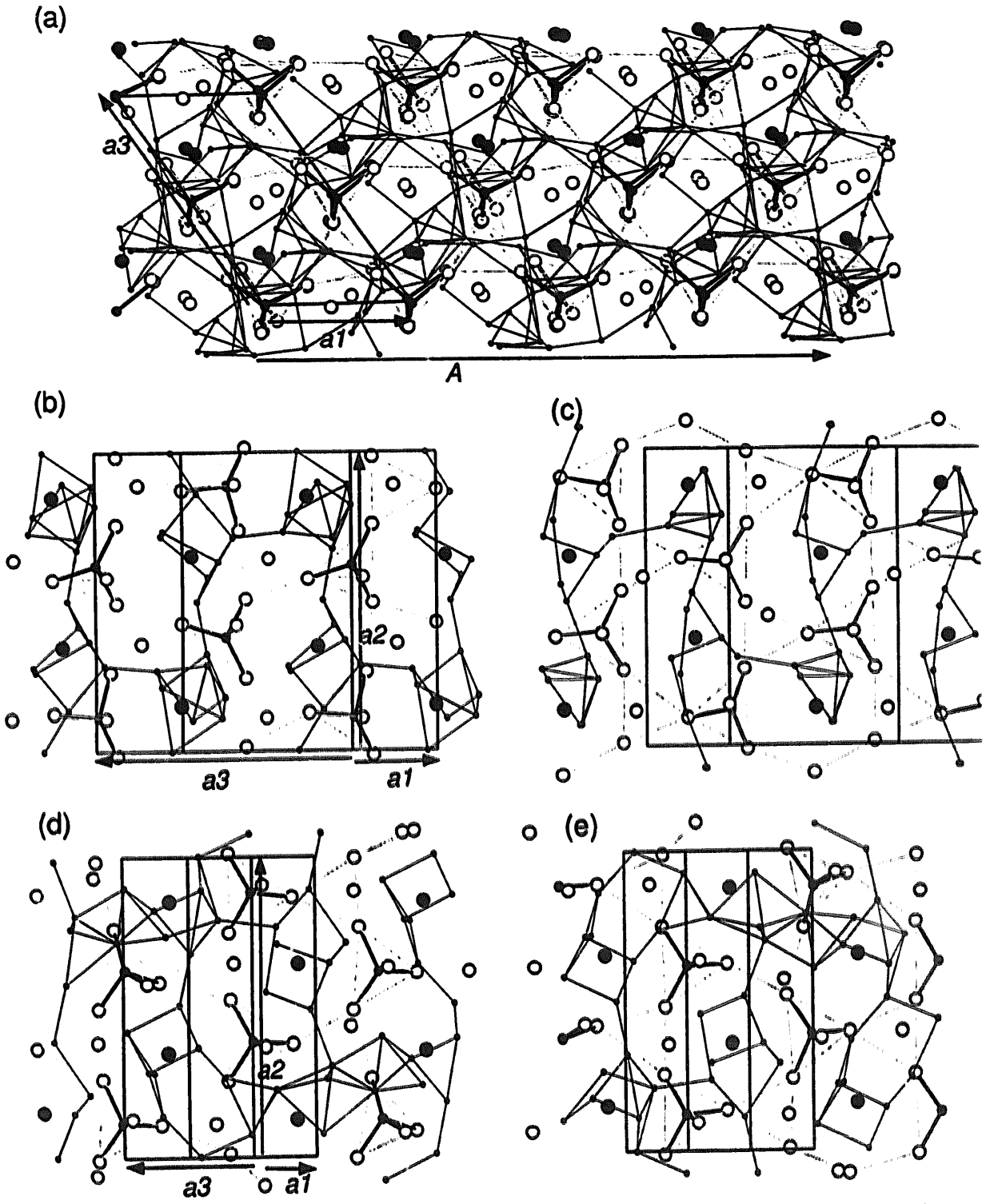

Fig. 2. Projections of the structure model of Ag_7NbS_6 II along (a) [0, 1, 0], (b,c) [−3, 0, −1], (d,e) [2, 0, −1] on the basis of the monoclinic unit cell of the fundamental structure ($a_1 = 7.368$ Å, $a_2 = 14.770$ Å, $a_3 = 12.768$ Å and $\beta = 124.28°$). The bounded areas for (b–e) are, respectively (b) $-0.23 < x < 0.77$, (c) $0.77 < x < 1.77$, (d) $-0.65 < x - 2z < 0.35$ and (e) $0.35 < x - 2z < 1.35$. Large open and hatched circles, medium solid circles and small solid circles represent S, Nb and Ag, respectively.

II were illustrated in Fig. 1 and Fig. 2. The selected interatomic distances of Ag_7NbS_6 II are shown in Table 3. In the model of Ag_7NbS_6 II, four independent Nb positions are present, and they are tetrahedral sites coordinated by S1, S2, S3 and S4 listed in Table 2. As shown in Fig. 2 and Table 3, 28 kinds of Ag sites are independent. Almost a half of Ag ions are in distorted S–S tetrahedrons formed by S5, S6 and two of S1, S2, S3 and S4. Most of the other half of Ag ions are in S–S triangular faces shared by two distorted tetrahedrons. The interatomic distances of Ag_7TaS_6 II listed in the previous paper [8] show that three of independent Ag ions are in the distorted S–S tetrahedrons and the residual four of Ag ions are in the triangles shared by two tetrahedrons.

In the approximate structure models [1,2] of the room-temperature phases Ag_7TaS_6 I and Ag_7NbS_6 I, mobile Ag ions are expressed as statistical distribution in many distorted S–S tetrahedrons and triangular faces shared by two distorted tetrahedrons. On cooling through approx. 280 K, the room-temperature phases are converted into low-temperature forms in which Ag ions stop into ordered arrangements. The ordered arrangement in Ag_7TaS_6 II is described in the monoclinic system with a space group Pc and a lattice constants a = 7.453 Å, b = 7.403 Å, c = 12.806 Å and $\beta = 124.62°$, and the Ag ion sites are three kinds of distorted tetrahedral sites and four kinds of triangular sites shared by two tetrahedrons. In the case of Ag_7NbS_6 II, the ordered arrangement is described in a large lattice with the monoclinic symmetry, that is A = 29.47 Å, B = 14.770 Å, C = 12.768 Å, $\beta = 124.28°$ with a space group Cc. The structure can be regarded as a commensurately and displacively modulated structure and the crystal data are expressed as $a_1 = 7.368$ Å, $a_2 = 14.770$ Å, $a_3 = 12.768$ Å, $\sigma = (0.25, 0, 0)$, $\beta = 124.28°$ in a four-dimensional formalism with a superspace-group $Pc(\alpha, 1/2, \gamma)$. The Ag ion sites in Ag_7NbS_6 II are distorted tetrahedral and triangular sites and their characters seem to be substantially similar to those of Ag_7TaS_6 II, although standard deviations listed in Table 2 are large due to the unfavorable data-to-parameter ratio.

In both Ag_7TaS_6 II and Ag_7NbS_6 II, Ag ions are coordinated by some others (Ag–Ag < 3.4 Å). They seem to form Ag clusters like deformed Ag–Ag networks. The Ag–Ag networks in Ag_7TaS_6 II seem to be parallel along $2\boldsymbol{a} + \boldsymbol{c}$ as shown in Fig. 1a,d,e and show a little anisotropic character, while the Ag–Ag networks in Ag_7NbS_6 II seem to have a more three-dimensional and deformed character (Fig. 2a–e). Symmetry lowering under approx. 280 K may be considered to arise by transferring of Ag ions from statistical distribution over many distorted S–S tetrahedrons and triangles shared by two tetrahedrons into a network-like arrangement described in the monoclinic system for Ag_7TaS_6 II or described in the monoclinic superstructure for Ag_7NbS_6 II.

Acknowledgements

The authors wish to express appreciation to Dr A. Yamamoto for his computer programs.

References

[1] H. Wada, M. Onoda, J. Less Common Met. 175 (1991) 209.
[2] H. Wada, J. Alloys Comp. 178 (1992) 315.
[3] W.F. Kuhs, R. Nitsche, K. Scheunemann, Acta Crystallogr. B34 (1978) 64.
[4] D. Carrè, R. Ollitrault-Fichet, J. Flahaut, Acta Crystallogr. B36 (1980) 245.
[5] M. Onoda, H. Wada, K. Yukino, M. Ishii, Solid State Ionics 79 (1995) 75.
[6] M. Onoda, M. Tansho, H. Wada, M. Ishii, Solid State Ionics 93 (1997) 297.
[7] M. Onoda, H. Wada, M. Ishii, Solid State Ionics 86/88 (1996) 217.
[8] A. Yamamoto, Acta Crystallogr. A48 (1992) 476.
[9] International Tables for X-ray Crystallography, Vol. C, 1992.